DMD Fast Forward. Published on September 27, 2011 as doi:10.1124/dmd.111.041400

CPY3A4-mediated lopinavir bioactivation and its inhibition by ritonavir

Feng Li, Jie Lu, and Xiaochao Ma

Department of Pharmacology, Toxicology and Therapeutics, University of Kansas Medical Center, Kansas City, Kansas

DMD Fast Forward. Published on September 27, 2011 as DOI: 10.1124/dmd.111.041400
This article has not been copyedited and formatted. The final version may differ from this version.

Running title: Lopinavir bioactivation and its inhibition by ritonavir

Corresponding Author: Xiaochao Ma, PhD, Department of Pharmacology, Toxicology and Therapeutics, University of Kansas Medical Center, Kansas City, Kansas 66160; Phone: (913) 588-1749; Fax: (913) 588-7501; Email: xma2@kumc.edu

Number of text pages: 26

Number of tables: 1

Number of figures: 8

Number of references: 31

Words in abstract: 140

Words in introduction: 356

Words in discussion: 597

Abbreviations: LPV, lopinavir; RTV, ritonavir; PI, protease inhibitor; LPV/r, ritonavir-boosted lopinavir regimen; DMP, 2,6-dimethylphenol; GSH, glutathione; HLM, human liver microsomes; PBS, phosphate-buffered saline; OPLS-DA, orthogonal projection to latent structures-discriminant analysis; TOFMS, time-of-flight mass spectrometry; UPLC, ultraperformance liquid chromatography.

DMD Fast Forward. Published on September 27, 2011 as DOI: 10.1124/dmd.111.041400
This article has not been copyedited and formatted. The final version may differ from this version.

Abstract

The combination of lopinavir (LPV) and ritonavir (RTV) is one of the preferred regimens for the treatment of HIV infection with confirmed efficacy and relatively low toxicity. LPV alone suffers the poor bioavailability due to its rapid and extensive metabolism. RTV boosts the plasma concentration of LPV by suppressing its metabolism and thus increasing LPV efficacy. In the current study, we found that RTV also inhibits LPV bioactivation. LPV bioactivation was investigated in human liver microsomes and cDNA-expressed human cytochromes P450. Twelve glutathione-trapped reactive metabolites of LPV were identified by using a metabolomic approach. Semicarbazide-trapped reactive metabolites of LPV were also detected. RTV effectively suppressed all pathways of LPV bioactivation via CYP3A4 inhibition. Our data together with previous reports suggest that LPV plus RTV is an ideal combination because RTV not only boosts LPV plasma concentration, but decreases LPV bioactivation.

DMD Fast Forward. Published on September 27, 2011 as DOI: 10.1124/dmd.111.041400
This article has not been copyedited and formatted. The final version may differ from this version.

Introduction

Lopinavir (LPV) is an HIV protease inhibitor (PI) (Sham et al., 1998; Hurst and Faulds, 2000). Because of the rapid metabolism of LPV by cytochrome P450 3A (CYP3A), LPV bioavailability is very low (Kumar et al., 1999a; Ter Heine et al., 2011). In clinical practice, LPV is co-administered with ritonavir (RTV), a PI that strongly inhibits CYP3A4 activity, to increase LPV plasma concentration and efficacy (Cvetkovic and Goa, 2003; Kumar et al., 2004; Oldfield and Plosker, 2006). In healthy volunteers, the maximum plasma concentration of LPV was shown to be ~0.1 mg/mL after a single dose of 400 mg LPV. In contrast, co-administration of 400 mg LPV with 50 mg RTV increased the maximum plasma concentration of LPV to 5.5 mg/mL (Sham et al., 1998). At present, the RTV-boosted LPV (LPV/r) regimen is the only co-formulated PI available that is approved by the Food and Drug Administration for the treatment of HIV infection in both adults and children (Croxtall and Perry, 2010).

The LPV/r regimen is generally well tolerated (Murphy et al., 2008; Gathe et al., 2009). For example, the incidence of severe liver events was relatively low in HIV patients receiving LPV/r (Bonfanti et al., 2005; Palacios et al., 2006). However, lead-in treatment with rifampicin significantly increased hepatotoxicity associated with LPV/r (Nijland et al., 2008). Rifampicin is a potent CYP3A inducer (Kolars et al., 1992), which may accelerate LPV and/or RTV bioactivation and result in liver injury. LPV is known to be metabolized by CYP3A (Kumar et al., 1999b; Kumar et al., 2004). Nevertheless, no information of LPV bioactivation is available. In a previous study, a mechanism-based inactivation of CYP3A4 by LPV has been reported (Ernest et al., 2005).

Mechanism-based P450 inactivation usually involves bioactivation of the drug to reactive intermediate(s), which covalently modify active site(s) of the P450 (Kalgutkar et al., 2007). These previous reports suggest that LPV bioactivation is likely occurring.

The current study was designed to investigate LPV bioactivation and examine the effect of RTV on LPV bioactivation. We identified glutathione (GSH)-trapped and semicarbazide-trapped reactive metabolites of LPV. RTV effectively inhibited all pathways of LPV bioactivation that are primarily mediated by CYP3A4.

Materials and methods

Materials. LPV [(2*S*)-*N*-[(2*S*,4*S*,5*S*)-5-[2-(2,6-dimethylphenoxy)acetamido]-4-hydroxy-1,6 diphenylhexan-2-yl]-3-methyl-2-(2-oxo-1,3-diazinan-1-yl)butanamide)] and RTV (1,3-thiazol-5-ylmethyl *N*-[(2*S*,3*S*,5*S*)-3-hydroxy-5-[(2*S*)-3-methyl-2-{[methyl({[2-(propan-2-yl)-1,3-thiazol-4-yl]methyl})carbamoyl]amino}butanamido]-1,6-diphenylhexan-2-yl]carbamate) were supplied by the National Institutes of Health AIDS Research and Reference Reagent Program. The recombinant human CYP450s and human liver microsomes (HLM) were purchased from XenoTech (Lenexa, KS). GSH, 2,6-dimethylphenol (DMP), semicarbazide and NADPH were obtained from Sigma-Aldrich (St. Louis, MO). All the solvents for liquid chromatography and mass spectrometry were of the highest grade commercially available.

LPV bioactivation. LPV bioactivation was investigated in HLM and cDNA-expressed human CYP450s. GSH and semicarbazide were used as trapping reagents to

confirm the existence of reactive metabolites of LPV. The incubation was conducted in 100 mM phosphate-buffered saline (PBS), containing 30 μM LPV, 2.5 mM GSH, 1.0 mg/mL HLM, and 1.0 mM NADPH in a final volume of 400 μL. The final volume of the incubation with semicarbazide (2.5 mM) was 1.5 mL. After 5 min of pre-incubation at 37 ˚C, the reaction was initiated by the addition of NADPH and continued for 50 min with gentle shaking. Incubations in the absence of NADPH or trapping reagent were used as controls. The reaction mixtures were quenched by adding 100 μL of formic acid (10% in water) for GSH containing incubations and 350 μL for the semicarbazide containing incubations. After centrifugation at 18,000 rcf for 10 min, the resulting supernatants were loaded onto Oasis HLB solid-phase extraction cartridges (Waters, Milford, MA). The cartridges were washed with 1.0 mL of water, followed by 1.0 mL of methanol. The methanol fractions were dried using nitrogen and reconstituted with 100 μL of acetonitrile/water (v/v, 50/50). Aliquots (5.0 μL) of the reconstituted solutions were injected into a system combining ultraperformance liquid chromatography (UPLC) and time-of-flight mass spectrometry (TOFMS) (SYNAPT G1, Waters, Milford, MA).

Effect of RTV on LPV bioactivation. Because LPV is co-administered with RTV in clinical practice, RTV was co-incubated with LPV to examine the effect of RTV on LPV bioactivation. The incubation was conducted in PBS (100 mM, pH 7.4), containing 30 μM LPV, 2.0 μM RTV, 2.5 mM GSH or semicarbazide, 1.0 mg/mL HLM. The reaction was initiated by the addition of NADPH and continued for 50 min with gentle shaking. The reaction mixtures were quenched by the addition of 10% formic acid. After

centrifugation at 18,000 rcf for 10 min, the resulting supernatants were extracted using solid-phase extraction cartridges and analyzed by UPLC-TOFMS.

Role of CYP450s in LPV bioactivation. cDNA-expressed CYP450s (CYP1A2, 2C8, 2C9, 2C19, 2D6, 2E1, and 3A4) were used to determine the role of individual CYP450 in LPV bioactivation. The incubation was conducted in PBS (100 mM, pH 7.4), containing 30 μM LPV, 2.5 mM GSH, and 10 pmol of each cDNA-expressed CYP450. The reaction was initiated by the addition of NADPH and continued for 50 min with gentle shaking. The reaction mixtures were quenched by the addition of 10% formic acid. After centrifugation at 18,000 rcf for 10 min, the resulting supernatants were extracted using solid-phase extraction cartridges and analyzed by UPLC-TOFMS. The incubations were conducted in duplicate.

Role of CYP450s in DMP bioactivation. DMP was identified as a novel metabolite of LPV in the current study. cDNA-expressed CYP450s were used to determine the role of individual CYP450 in DMP bioactivation. The incubation was conducted in PBS (100 mM, pH 7.4), containing 30 μM DMP, 2.5 mM GSH, and 20 pmol of each cDNA-expressed CYP450 in a final volume of 200 μL. The reaction was initiated by adding of NADPH and continued for 30 min with gentle shaking. The reaction mixtures were terminated by the addition of cold acetonitrile (200 μL). After centrifugation at 18,000 rcf for 10 min, the resulting supernatants were analyzed by UPLC-TOFMS. The incubations were conducted in duplicate.

DMD Fast Forward. Published on September 27, 2011 as DOI: 10.1124/dmd.111.041400
This article has not been copyedited and formatted. The final version may differ from this version.

UPLC-TOFMS analyses. Chromatographic separation of trapped reactive metabolites of LPV was achieved using a 100 mm x 2.1 mm (Acquity 1.7 µm) UPLC BEH C-18 column (Waters, Milford, MA). The flow rate of the mobile phase was 0.3 mL/min with a gradient ranging from 2% to 98% aqueous acetonitrile containing 0.1% formic acid in a 10-min run. TOFMS was operated in a positive mode with electrospray ionization. The source temperature and desolvation temperature were set at 120 °C and 350 °C, respectively. Nitrogen was applied as the cone gas (10 liters/hour), and desolvation gas (700 liters/hour). Argon was applied as the collision gas. TOFMS was calibrated with sodium formate and monitored by the intermittent injection of lock mass leucine enkeophalin in real time, generating a reference ion at *m/z* 556.2771. The capillary voltage and the cone voltage were set at 3.5 kV and 35 V. The structures of trapped reactive metabolites of LPV were elucidated by tandem mass spectrometry fragmentation with collision energy ramp ranging from 10 to 40 eV.

Data analysis. The implication of a metabolomic approach in studying xenobiotics bioactivation was recently developed and verified by examining bioactivation of pulegone, acetaminophen, and clozapine (Li et al., 2011). Briefly, mass chromatograms and mass spectra were acquired by MassLynx software (Waters Corp., Milford, MA) in centroid format from *m/z* 50 to 1000. Centroid and integrated mass chromatographic data were processed by MarkerLynx software (Waters Corp., Milford, MA) to generate a multivariate data matrix. The corresponding data matrices were then exported into SIMCA-P (Umetrics, Kinnelon, NJ) for multivariate data analysis. Principal component analysis and orthogonal projection to latent structures-discriminant analysis (OPLS-DA)

DMD Fast Forward. Published on September 27, 2011 as DOI: 10.1124/dmd.111.041400
This article has not been copyedited and formatted. The final version may differ from this version.

were conducted on Pareto-scaled data. For chemometric analysis, the matrix data were processed from *m/z* 700 to 1000.

Results

Profiling trapped reactive metabolites of LPV using a metabolomic approach. Overall, 12 GSH-trapped and 3 semicarbazide-trapped reactive metabolites of LPV were identified (Table 1). The results of chemometric analysis of the incubations of LPV in HLM are shown in Figure 1. The supervised OPLS-DA analysis separated samples corresponding to two controls (without GSH or NADPH) and the analyte (with GSH and NADPH) (Figure 1A). The S-plot generated from OPLS-DA analysis revealed that LPV_GSH adducts highly contributed to the group separation (Figure 1B). Ten LPV_GSH adducts (I-X) were readily uncovered, including two GSH conjugated LPV adducts (I and II), four GSH conjugated monohydroxylated LPV adducts (III, IV, V, and VI), one GSH conjugated dihydroxylated+dehydrogenated LPV adduct (VII), one GSH conjugated dihydroxylated LPV adduct (VIII), and two GSH conjugated trihydroxylated+ dehydrogenated LPV adducts (IX and X). In addition, two GSH conjugated hydroxylated DMP adducts (XI and XII) and three LPV_semicarbazide adducts (LPV_hydrazones 1, 2 and 3) were screened out from the biological matrix as expected metabolites.

Identification of GSH-trapped reactive metabolites of LPV. Structural elucidations were performed on the basis of accurate mass measurement and MS/MS fragmentations. LPV adduct I, eluted at 5.73 min (Figure 2A), had a protonated molecule $[M+H]^+$ at *m/z* 934.4413, 305 Daltons higher than that of LPV. Compared to the MS/MS

of LPV (Figure 2B), adduct I had the same fragments at *m/z* 447.2668 and 429.2541, suggesting that GSH conjugated at the right moiety. The fragment ion at *m/z* 488.1823 in Figure 2C is 305 Daltons higher than that of ion at 183 in Figure 2B, indicating that the GSH moiety was attached to the encircled unit (Figure 2C). Other fragments were interpreted in the inlaid structural diagram. Adduct II was eluted at 5.68 min (Figure 2A), having a protonated molecule $[M+H]^+$ at *m/z* 934.4384 (Figure 2D). Adduct II had similar mass spectra patterns to that of adduct I, indicating that GSH was linked to the same unit as with adduct I, but at a different position. The chromatograms and MS/MS spectra of LPV_GSH adducts III to X are provided in the supplemental data (Supplemental Figures 1 to 4).

Identification of semicarbazide-trapped reactive metabolites of LPV. Three LPV hydrazones (LPV_hydrazone_1, 2, and 3) were detected in the incubation of LPV with semicarbazide in HLM (Figure 3). LPV_hydrazone_1, eluted at 4.99 min (Figure 3A), had a protonated molecule $[M+H]^+$ at *m/z* 580.3199. MS/MS analysis of LPV_hydrazone_1 produced daughter ions at *m/z* 398.2188, 323.1753, 183.1134, and 155.1183 (Figure 3B). The mass difference between the ions at *m/z* 398.2188 and 323.1753 is 75 Daltons, which equals to the mass of semicarbazide, suggesting that hydrazone formed. LPV_hydrazone_2 (Figures 3A and 3C), eluted at 4.58 min, had a protonated molecule $[M+H]^+$ at *m/z* 578.3071. MS/MS analysis of LPV_hydrazone_2 produced daughter ions at *m/z* 560.3050 (loss of H_2O), 398.2188, 323.1764, 181.1008, and 153.1023. Compared to the ions at *m/z* 183.1134 and 155.1183 generated from LPV_hydrazone_1, the ions at 181.1008 and 153.1023 from LPV_hydrazone_2 indicate

that the dehydrogenation occurred in the encircled units (Figure 3C). LPV_hydrazone_3 had a protonated molecule $[M+H]^+$ at *m/z* 594.3044, 16 Daltons higher than that of LPV_hydrazone_2. MS/MS analysis of LPV_hydrazone_3 produced daughter ions at *m/z* 576.2954 (loss of H_2O), 398.2197, 381.1949, 323.1733, and 250.1614. Compared to the ions at *m/z* 181.1008 and 153.1023 produced from LPV_hydrazone_2, the ions at 197.0921 and 169.0972 from LPV_hydrazone_3 suggest that the dehydrogenation and hydroxylation occurred in the encircled units (Figure 3D).

Coupled with the generation of LPV aldehydes, DMP is produced (Figure 4). DMP is further oxidized to form O_DMP, which can be transformed into reactive intermediates, such as quinone and/or quinone methide, and then be trapped by GSH (Evans et al., 2004; Ma and Subramanian, 2006). In the incubation of LPV in HLM containing GSH, two GSH conjugated DMP adducts were identified (Figure 5). Adduct XI was detected at 3.22 min (Figure 5A), having a protonated molecule $[M+H]^+$ at *m/z* 444.1396. The MS/MS of adduct XI produced fragment ions at *m/z* 315.1006, 195.0494, 169.0330, and 130.0508. The formation of ions 315.1006 and 169.0330 suggest that the GSH was connected to monooxidized DMP (Figure 5B). Adduct XII, eluted at 2.98 min (Figure 5A), had a protonated molecule $[M+H]^+$ at *m/z* 444.1425. Adduct XII had a similar fragmentation pattern to that of XI, except for the ions at *m/z* 297.0750 and 251.0679. The slight difference in MS/MS between XI and XII suggest that the hydroxylated or GSH coupled position varied (Figure 5C). The existence of adducts XI and XII were confirmed in the incubation of authentic DMP in HLM containing GSH (data not shown).

DMD Fast Forward. Published on September 27, 2011 as DOI: 10.1124/dmd.111.041400
This article has not been copyedited and formatted. The final version may differ from this version.

Effect of RTV on LPV bioactivation. Twelve GSH conjugated LPV adducts were identified in the incubation with HLM (Figure 6). RTV significantly suppressed all pathways of LPV bioactivation. The formation of LPV adducts I and II was suppressed ~80% by RTV in the incubation with HLM (Figure 6). The formations of LPV_GSH adducts III to XII were completely inhibited by RTV (Figure 6). The formations of semicarbazide conjugated LPV adducts (LPV_Hydrazone_1, 2, and 3) were also entirely inhibited by RTV (Figure 7). These data suggest that CYP3A4 plays an important role in the LPV bioactivation and RTV suppresses LPV bioactivation via CYP3A4 inhibition.

Role of CYP450s in LPV bioactivation. From the inhibitory test of RTV on LPV bioactivation, we observed that RTV cannot entirely suppress LPV adducts I and II formation in HLM (Figure 6), suggesting that some other enzyme(s) are involved in LPV bioactivation. We examined LPV bioactivation in a panel of CYP450s including CYP1A2, 2C8, 2C9, 2C19, 2D6, 2E1, and 3A4. CYP3A4 was identified as the dominant enzyme in the formation of LPV adducts I and II. In addition, ~8% of the formation of LPV adducts I and II was mediated by CYP2D6 (Figure 8A). These data suggest that CYP2D6 may be involved in LPV bioactivation. We found that multiple enzymes, especially CYP1A2, are involved in DMP bioactivation (Figure 8B). These data suggest that the formation of adducts XI and XII need two metabolic steps (Figure 4): step 1 is primarily mediated by CYP3A4 and step 2 is primarily mediated by CYP1A2.

DMD Fast Forward. Published on September 27, 2011 as DOI: 10.1124/dmd.111.041400
This article has not been copyedited and formatted. The final version may differ from this version.

Discussion

Characterizing reactive intermediates can provide information on the structure of the reactive species, thereby defining a potential bioactivation mechanism. In addition, information on adducts of reactive metabolites can be used to predict the potential bindings of reactive metabolites with cellular proteins and/or some other molecules. Most reactive metabolites are not stable, so it is difficult to detect them directly. Reactive metabolites can form adducts with trapping reagents that make the reactive metabolites detectable (Evans et al., 2004; Li et al., 2011). GSH is commonly used to trap soft electrophiles, such as epoxides, α,β-unsaturated carbonyls, quinones, quinone imines, quinone methides, imine methide, isocyanate, isothiocynates, aziridinium, and episulfonium (Evans et al., 2004; Ma and Subramanian, 2006). Semicarbazide is used to trap hard electrophiles, such as aldehydes (Evans et al., 2004; Li et al., 2011). In the current study, GSH and semicarbazide were used as trapping reagents. We identified 12 GSH-trapped and 3 semicarbazide-trapped reactive metabolites of LPV.

Our study showed that CYP3A4 is the primary enzyme involved in LPV bioactivation (Figures 6 and 7). CYP3A4 is one of the most important metabolic enzymes expressed in liver and intestine (Guengerich, 1999). Induction or inhibition of CYP3A4 has been known to cause significant drug-drug interactions (Guengerich, 1997; Tanaka, 1998). Because of the importance of CYP3A4 in LPV bioactivation, the effects of CYP3A4 inhibitors and inducers on LPV bioactivation are expected. RTV is a potent CYP3A4 inhibitor that is routinely co-administered with LPV. We found that RTV effectively suppressed LPV bioactivation (Figures 6 and 7). To our knowledge, no clinical studies

DMD Fast Forward. Published on September 27, 2011 as DOI: 10.1124/dmd.111.041400
This article has not been copyedited and formatted. The final version may differ from this version.

have been done to compare the safety profile of LPV/r to LPV alone. However, there is a case report in which LPV alone caused serious multi-organ hypersensitivity (Manfredi and Sabbatani, 2006). These data suggest that RTV may reduce the toxic risk resulting from LPV bioactivation.

On the contrary, co-administering a CYP3A4 inducer, such as rifampicin, with LPV may increase LPV bioactivation and augment LPV side effects. Previous clinical studies have demonstrated that rifampicin decreases the plasma concentration of LPV (la Porte et al., 2004; Ren et al., 2008) and increases the incidence of LPV/r hepatotoxicity (Nijland et al., 2008; L'Homme R et al., 2009). Further studies are suggested to determine the role of rifampicin-mediated CYP3A4 induction in LPV/r bioactivation and hepatotoxicity.

In addition to CYP3A4, we noted that CYP2D6 and 1A2 also contribute to LPV bioactivation. CYP2D6 is involved in the formation of adducts I, II, XI, and XII (Figure 8). Although CYP2D6 plays a minor role in these pathways of LPV bioactivation, CYP2D6 cannot be neglected because of the extremely high polymorphism of this enzyme (Ingelman-Sundberg, 2005). DMP is a metabolite of LPV that can be further metabolized to form quinone and/or quinone methide intermediates that are known to be toxic mediators in drug-induced toxicity (Bolton et al., 2000; Evans et al., 2004). We trapped these intermediates by using GSH. CYP1A2 is determined to be the primary enzyme contributing to DMP bioactivation (Figures 8B). CYP1A2 expression is highly inducible by a number of dietary components and some polycyclic aromatic hydrocarbons, some of which are found in cigarette smoke (Kalow and Tang, 1991;

Sachse et al., 2003). Therefore, smoking and CYP1A2 inducers should be avoided in patients treated with LPV/r, especially in the condition of CYP3A4 induction.

In summary, LPV bioactivation was investigated using a metabolomic approach. Twelve GSH-trapped and three semicarbazide-trapped reactive metabolites of LPV were identified. RTV effectively suppressed LPV bioactivation via CYP3A4 inhibition. Our data together with previous reports suggest that LPV/r is an ideal combination because RTV not only boosts LPV plasma concentration, but decreases LPV bioactivation.

Acknowledgements

We thank the National Institutes of Health AIDS Research and Reference Reagent Program for providing the HIV protease inhibitors. We thank Dr. Martha Montello for editing the manuscript.

Authorship contributions

Participated in research design: Feng Li, Xiaochao Ma

Conducted experiments: Feng Li, Jie Lu

Contributed the new reagents or analytic tools: Feng Li

Performed data analysis: Feng Li, Xiaochao Ma

Wrote or contributed to the writing of manuscript: Feng Li, Xiaochao Ma

References

Bolton JL, Trush MA, Penning TM, Dryhurst G and Monks TJ (2000) Role of quinones in toxicology. *Chem Res Toxicol* **13:**135-160.

Bonfanti P, Ricci E, Penco G, Orofino G, Bini T, Sfara C, Miccolis S, Cristina G and Quirino T (2005) Low incidence of hepatotoxicity in a cohort of HIV patients treated with lopinavir/ritonavir. *AIDS* **19:**1433-1434.

Croxtall JD and Perry CM (2010) Lopinavir/Ritonavir: a review of its use in the management of HIV-1 infection. *Drugs* **70:**1885-1915.

Cvetkovic RS and Goa KL (2003) Lopinavir/ritonavir: a review of its use in the management of HIV infection. *Drugs* **63:**769-802.

Ernest CS, 2nd, Hall SD and Jones DR (2005) Mechanism-based inactivation of CYP3A by HIV protease inhibitors. *J Pharmacol Exp Ther* **312:**583-591.

Evans DC, Watt AP, Nicoll-Griffith DA and Baillie TA (2004) Drug-protein adducts: an industry perspective on minimizing the potential for drug bioactivation in drug discovery and development. *Chem Res Toxicol* **17:**3-16.

Gathe J, da Silva BA, Cohen DE, Loutfy MR, Podzamczer D, Rubio R, Gibbs S, Marsh T, Naylor C, Fredrick L and Bernstein B (2009) A once-daily lopinavir/ritonavir-based regimen is noninferior to twice-daily dosing and results in similar safety and tolerability in antiretroviral-naive subjects through 48 weeks. *J Acquir Immune Defic Syndr* **50:**474-481.

Guengerich FP (1997) Role of cytochrome P450 enzymes in drug-drug interactions. *Adv Pharmacol* **43:**7-35.

Guengerich FP (1999) Cytochrome P-450 3A4: regulation and role in drug metabolism. *Annu Rev Pharmacol Toxicol* **39:**1-17.

Hurst M and Faulds D (2000) Lopinavir. *Drugs* **60:**1371-1379; discussion 1380-1371.

Ingelman-Sundberg M (2005) Genetic polymorphisms of cytochrome P450 2D6 (CYP2D6): clinical consequences, evolutionary aspects and functional diversity. *Pharmacogenomics J* **5:**6-13.

Kalgutkar AS, Obach RS and Maurer TS (2007) Mechanism-based inactivation of cytochrome P450 enzymes: chemical mechanisms, structure-activity relationships and relationship to clinical drug-drug interactions and idiosyncratic adverse drug reactions. *Curr Drug Metab* **8:**407-447.

Kalow W and Tang BK (1991) Caffeine as a metabolic probe: exploration of the enzyme-inducing effect of cigarette smoking. *Clin Pharmacol Ther* **49:**44-48.

Kolars JC, Schmiedlin-Ren P, Schuetz JD, Fang C and Watkins PB (1992) Identification of rifampin-inducible P450IIIA4 (CYP3A4) in human small bowel enterocytes. *J Clin Invest* **90:**1871-1878.

Kumar GN, Dykstra J, Roberts EM, Jayanti VK, Hickman D, Uchic J, Yao Y, Surber B, Thomas S and Granneman GR (1999a) Potent inhibition of the cytochrome P-450 3A-mediated human liver microsomal metabolism of a novel HIV protease inhibitor by ritonavir: A positive drug-drug interaction. *Drug Metab Dispos* **27:**902-908.

Kumar GN, Jayanti V, Lee RD, Whittern DN, Uchic J, Thomas S, Johnson P, Grabowski B, Sham H, Betebenner D, Kempf DJ and Denissen JF (1999b) In vitro

metabolism of the HIV-1 protease inhibitor ABT-378: species comparison and metabolite identification. *Drug Metab Dispos* **27:**86-91.

Kumar GN, Jayanti VK, Johnson MK, Uchic J, Thomas S, Lee RD, Grabowski BA, Sham HL, Kempf DJ, Denissen JF, Marsh KC, Sun E and Roberts SA (2004) Metabolism and disposition of the HIV-1 protease inhibitor lopinavir (ABT-378) given in combination with ritonavir in rats, dogs, and humans. *Pharm Res* **21:**1622-1630.

L'Homme R F, Nijland HM, Gras L, Aarnoutse RE, van Crevel R, Boeree M, Brinkman K, Prins JM, Juttmann JR and Burger DM (2009) Clinical experience with the combined use of lopinavir/ritonavir and rifampicin. *AIDS* **23:**863-865.

la Porte CJ, Colbers EP, Bertz R, Voncken DS, Wikstrom K, Boeree MJ, Koopmans PP, Hekster YA and Burger DM (2004) Pharmacokinetics of adjusted-dose lopinavir-ritonavir combined with rifampin in healthy volunteers. *Antimicrob Agents Chemother* **48:**1553-1560.

Li F, Lu J and Ma X (2011) Profiling the reactive metabolites of xenobiotics using metabolomic technologies. *Chem Res Toxicol* **24:**744-751.

Ma S and Subramanian R (2006) Detecting and characterizing reactive metabolites by liquid chromatography/tandem mass spectrometry. *J Mass Spectrom* **41:**1121-1139.

Manfredi R and Sabbatani S (2006) Serious, multi-organ hypersensitivity to lopinavir alone, involving cutaneous-mucous rash, and myeloid, liver, and kidney function. *AIDS* **20:**2399-2400.

Murphy RL, da Silva BA, Hicks CB, Eron JJ, Gulick RM, Thompson MA, McMillan F, King MS, Hanna GJ and Brun SC (2008) Seven-year efficacy of a lopinavir/ritonavir-based regimen in antiretroviral-naive HIV-1-infected patients. *HIV Clin Trials* **9:**1-10.

Nijland HM, L'Homme R F, Rongen GA, van Uden P, van Crevel R, Boeree MJ, Aarnoutse RE, Koopmans PP and Burger DM (2008) High incidence of adverse events in healthy volunteers receiving rifampicin and adjusted doses of lopinavir/ritonavir tablets. *AIDS* **22:**931-935.

Oldfield V and Plosker GL (2006) Lopinavir/ritonavir: a review of its use in the management of HIV infection. *Drugs* **66:**1275-1299.

Palacios R, Vergara S, Rivero A, Aguilar I, Macias J, Camacho A, Lozano F, Garcia-Lazaro M, Pineda JA, Torre-Cisneros J, Marquez M and Santos J (2006) Low incidence of severe liver events in HIV patients with and without hepatitis C or B coinfection receiving lopinavir/ritonavir. *HIV Clin Trials* **7:**319-323.

Ren Y, Nuttall JJ, Egbers C, Eley BS, Meyers TM, Smith PJ, Maartens G and McIlleron HM (2008) Effect of rifampicin on lopinavir pharmacokinetics in HIV-infected children with tuberculosis. *J Acquir Immune Defic Syndr* **47:**566-569.

Sachse C, Bhambra U, Smith G, Lightfoot TJ, Barrett JH, Scollay J, Garner RC, Boobis AR, Wolf CR and Gooderham NJ (2003) Polymorphisms in the cytochrome P450 CYP1A2 gene (CYP1A2) in colorectal cancer patients and controls: allele frequencies, linkage disequilibrium and influence on caffeine metabolism. *Br J Clin Pharmacol* **55:**68-76.

Sham HL, Kempf DJ, Molla A, Marsh KC, Kumar GN, Chen CM, Kati W, Stewart K, Lal R, Hsu A, Betebenner D, Korneyeva M, Vasavanonda S, McDonald E, Saldivar A, Wideburg N, Chen X, Niu P, Park C, Jayanti V, Grabowski B, Granneman GR, Sun E, Japour AJ, Leonard JM, Plattner JJ and Norbeck DW (1998) ABT-378, a highly potent inhibitor of the human immunodeficiency virus protease. *Antimicrob Agents Chemother* **42:**3218-3224.

Tanaka E (1998) Clinically important pharmacokinetic drug-drug interactions: role of cytochrome P450 enzymes. *J Clin Pharm Ther* **23:**403-416.

Ter Heine R, Van Waterschoot RA, Keizer RJ, Beijnen JH, Schinkel AH and Huitema AD (2011) An integrated pharmacokinetic model for the influence of CYP3A4 expression on the in vivo disposition of lopinavir and its modulation by ritonavir. *J Pharm Sci* **100:**2508-2515.

Footnote

This work was supported by the National Institutes of Health National Center for Research Resources [COBRE 5P20-RR021940].

DMD Fast Forward. Published on September 27, 2011 as DOI: 10.1124/dmd.111.041400
This article has not been copyedited and formatted. The final version may differ from this version.

FIGURE LEGENDS

Figure 1. Metabolomic analysis of control groups and GSH trapped group of LPV in the incubations with HLM. The incubation conditions of LPV were detailed in experimental procedures. All samples were analyzed by UPLC-TOFMS. (A) Separation of each incubation group in OPLS-DA score plot. The t[1]P and t[2]O values represent the score of each sample in principal component 1 and 2, respectively. (B) Loading S-plot generated by OPLS-DA analysis. The *X*-axis is a measure of the relative abundance of ions and the *Y*-axis is a measure of the correlation of each ion to the model. The top ranking ions are labeled. *, in-source fragment.

Figure 2. Identification of GSH conjugated LPV adducts I and II. LPV was incubated in HLM containing GSH and analyzed by UPLC-TOFMS. Major daughter ions from fragmentation were interpreted in the inlaid structural diagrams. (A) Extracted ion chromatograms of LPV adducts I and II. (B) MS/MS of LPV. (C) MS/MS of LPV adduct I. (D) MS/MS of LPV adduct II.

Figure 3. The extracted ion chromatograms (A) and MS/MS spectra of LPV_hydrazone_1 (B), 2 (C), and 3 (D). Three LPV hydrazones (LPV_hydrazone_1, 2 and 3) were detected in the incubation of LPV in HLM containing semicarbazide. All samples were analyzed by UPLC-TOFMS. Major daughter ions from fragmentation were interpreted in the inlaid structural diagrams.

Figure 4. Proposed mechanism of the formation of aldehydes and DMP in LPV metabolism, and the strategies to trap these metabolites.

Figure 5. Identification of GSH conjugated DMP adducts XI and XII. The incubation conditions of LPV were detailed in experimental procedures. All samples were analyzed by UPLC-TOFMS. Major daughter ions from fragmentation were interpreted in the inlaid structural diagrams. (A) Extracted ion chromatograms of adducts XI and XII. (B) MS/MS of adduct XI. (C) MS/MS of adduct XII.

Figure 6. Effect of RTV on the formation of GSH conjugated LPV adducts. Quadruplicate incubations were conducted in PBS (pH 7.4) containing LPV (30 μM), GSH (2.5 mM), NADPH (1.0 mM), HLM (1.0 mg/ml). RTV (2.0 μM) was used in the inhibitory test. All samples were analyzed by UPLC-TOFMS. The abundance of each adduct was relatively quantified using peak areas and presented as mean ± SD. ND, not detected.

Figure 7. Effect of RTV on the formation of semicarbazide conjugated LPV adducts. Duplicate incubations were conducted in PBS (pH 7.4) containing LPV (30 μM), semicarbazide (2.5 mM), NADPH (1.0 mM), HLM (1.0 mg/ml). RTV (2.0 μM) was used in the inhibitory test. All samples were analyzed by UPLC-TOFMS. The abundance of each adduct was relatively quantified using peak areas and presented as mean. ND, not detected.

DMD Fast Forward. Published on September 27, 2011 as DOI: 10.1124/dmd.111.041400
This article has not been copyedited and formatted. The final version may differ from this version.

Figure 8. Role of CYP450s in LPV bioactivation. cDNA-expressed CYP450s were used to determine the role of individual CYP450 in LPV bioactivation. The incubation conditions of LPV were detailed in experimental procedures. All samples were analyzed by UPLC-TOFMS. (A) Enzymes contributing to the formation of LPV adducts I and II. The substrate was LPV. The peak area of each adduct from the incubation with CYP3A4 was set as 100%. (B) Enzymes contributing to the formation of adducts XI and XII. The substrate was DMP. The peak area of each adduct from the incubation with CYP1A2 was set as 100%. All data are expressed as mean (n=2). ND, not detected.

Table 1. Summary of trapped reactive metabolites of LPV*.

Mass	Predicted formula	RT (min)	Mass error (ppm)	Identification	Code
934.4430	$C_{47}H_{64}N_7O_{11}S$	5.73	4.8	LPV_GSH	I
934.4443	$C_{47}H_{64}N_7O_{11}S$	5.68	6.2	LPV_GSH	II
950.4378	$C_{47}H_{64}N_7O_{12}S$	5.81	4.6	O_LPV_GSH	III
950.4404	$C_{47}H_{64}N_7O_{12}S$	5.65	7.4	O_LPV_GSH	IV
950.4346	$C_{47}H_{64}N_7O_{12}S$	5.11	1.3	O_LPV_GSH	V
950.4398	$C_{47}H_{64}N_7O_{12}S$	5.00	5.2	O_LPV_GSH	VI
964.4189	$C_{47}H_{62}N_7O_{13}S$	4.66	6.5	2O_LPV_GSH (-2H)	VII
966.4221	$C_{47}H_{64}N_7O_{13}S$	5.03	-6.3	2O_LPV_GSH	VIII
980.4088	$C_{47}H_{62}N_7O_{14}S$	4.70	1.3	3O_LPV_GSH (-2H)	IX
980.4104	$C_{47}H_{62}N_7O_{14}S$	4.78	3.0	3O_LPV_GSH (-2H)	X
444.1468	$C_{18}H_{26}N_3O_8S$	3.22	6.1	O_DMP_GSH	XI
444.1460	$C_{18}H_{26}N_3O_8S$	2.98	4.3	O_DMP_GSH	XII
580.3259	$C_{30}H_{42}N_7O_5$	4.99	2.1	LPV_aldehyde_semicarbazide	LPV_hydrazone_1

578.3099	$C_{30}H_{40}N_7O_5$	4.58	1.4	LPV_aldehyde_semicarbazide (-2H)	LPV_hydrazone_2
594.3040	$C_{30}H_4N_7O_6$	4.74	0.5	O_LPV_aldehyde_semicarbazide (-2H)	LPV_hydrazone_3

*The incubation conditions of LPV were detailed in experimental procedures. All samples were analyzed by UPLC-TOFMS. RT, retention time; O, monohydroxylated; 2O, dihydroxylated; 3O, trihydroxylated; -2H, dehydrogenated.

Figure 1

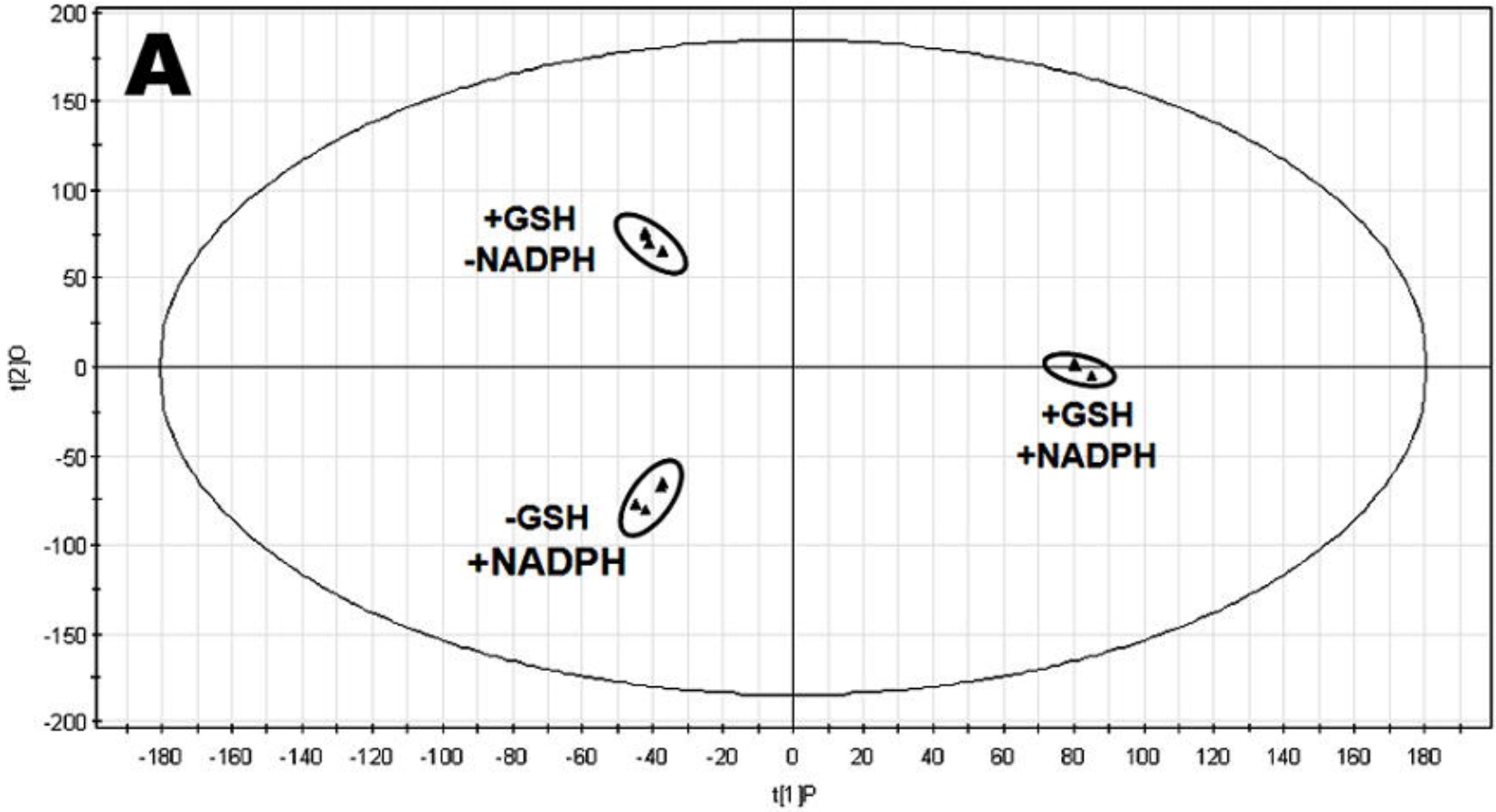
A
+GSH
-NADPH
+GSH
+NADPH
-GSH
+NADPH
t[2]O
t[1]P

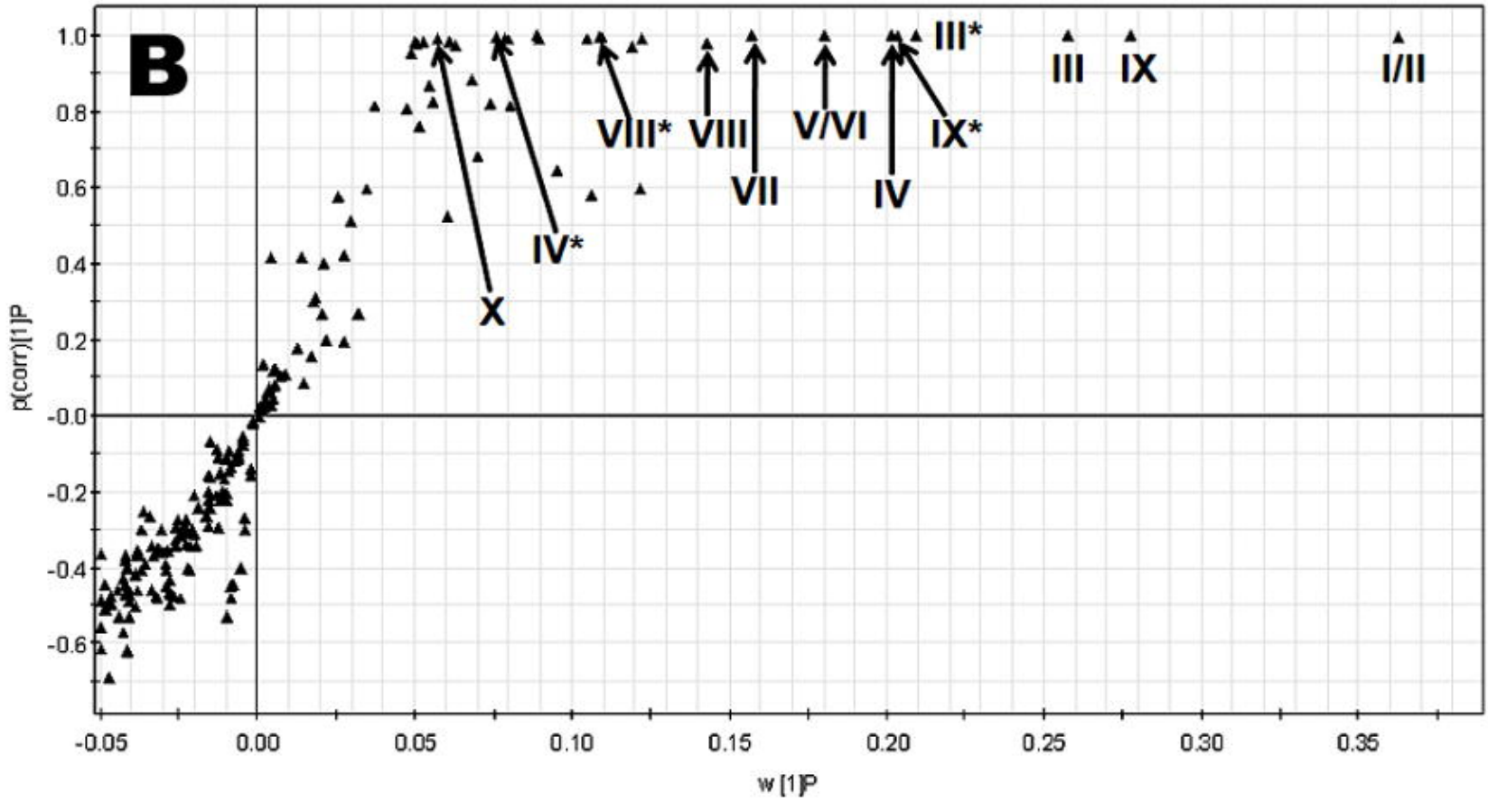
B
III*
III
IX
I/II
VIII*
VIII
V/VI
IX*
VII
IV
IV*
X
p(corr)[1]P
w [1]P

Figure 2

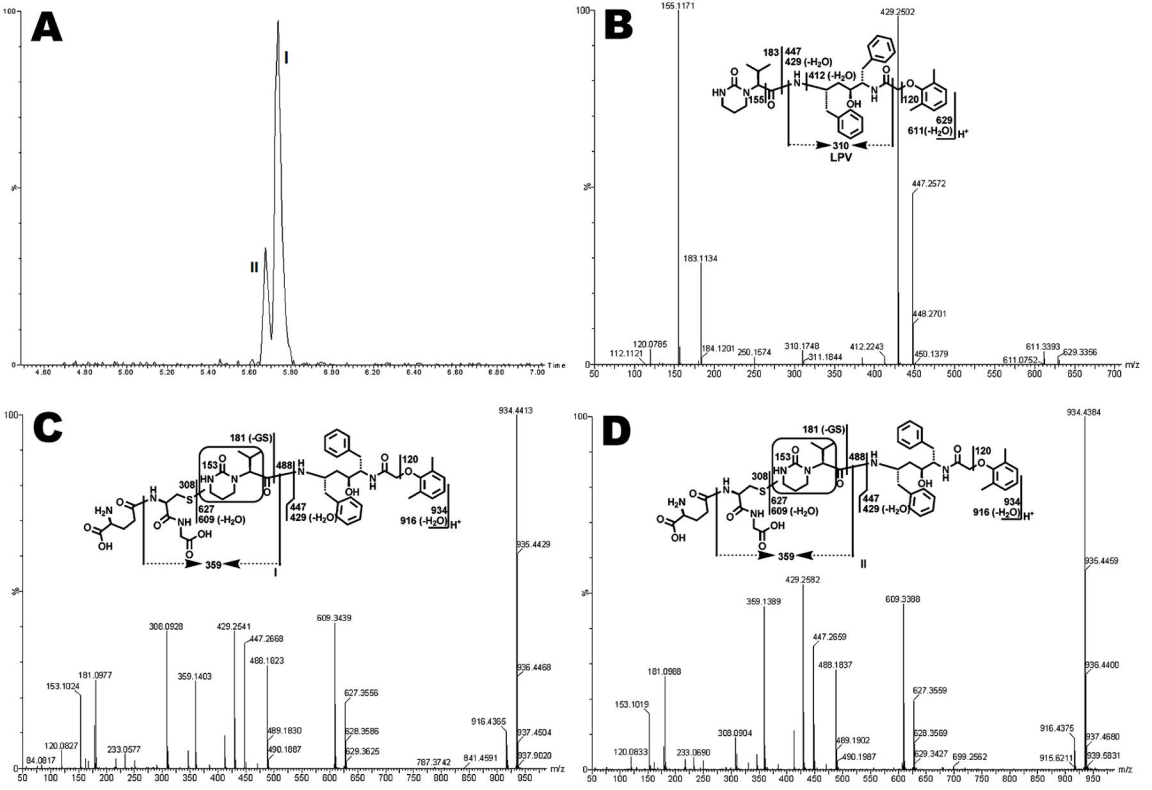
A
I
II
Time
B
155.1171
429.2502
447.2572
183.1134
448.2701
120.0765
184.1201
250.1574
310.1748
311.1844
412.2243
450.1379
611.3393
629.3356
611.0752
183
447
429 (-H2O)
412 (-H2O)
155
H20
629
611(-H2O) H+
310
LPV
C
934.4413
935.4429
936.4468
937.4504
937.9020
308.0928
429.2541
447.2668
488.1623
609.3439
359.1403
627.3556
181.0977
153.1024
489.1830
628.3586
490.1887
916.4365
629.3625
120.0827
84.0817
233.0577
787.3742
841.4591
181 (-GS)
153
308
627
609 (-H2O)
359
I
488
447
429 (-H2O)
120
934
916 (-H2O) H+
D
934.4384
935.4459
936.4400
937.4680
939.5831
429.2582
359.1389
609.3398
447.2659
488.1837
627.3559
181.0968
153.1019
489.1902
628.3569
490.1987
916.4375
629.3427
120.0833
233.0690
699.2562
915.6211
II

Figure 3

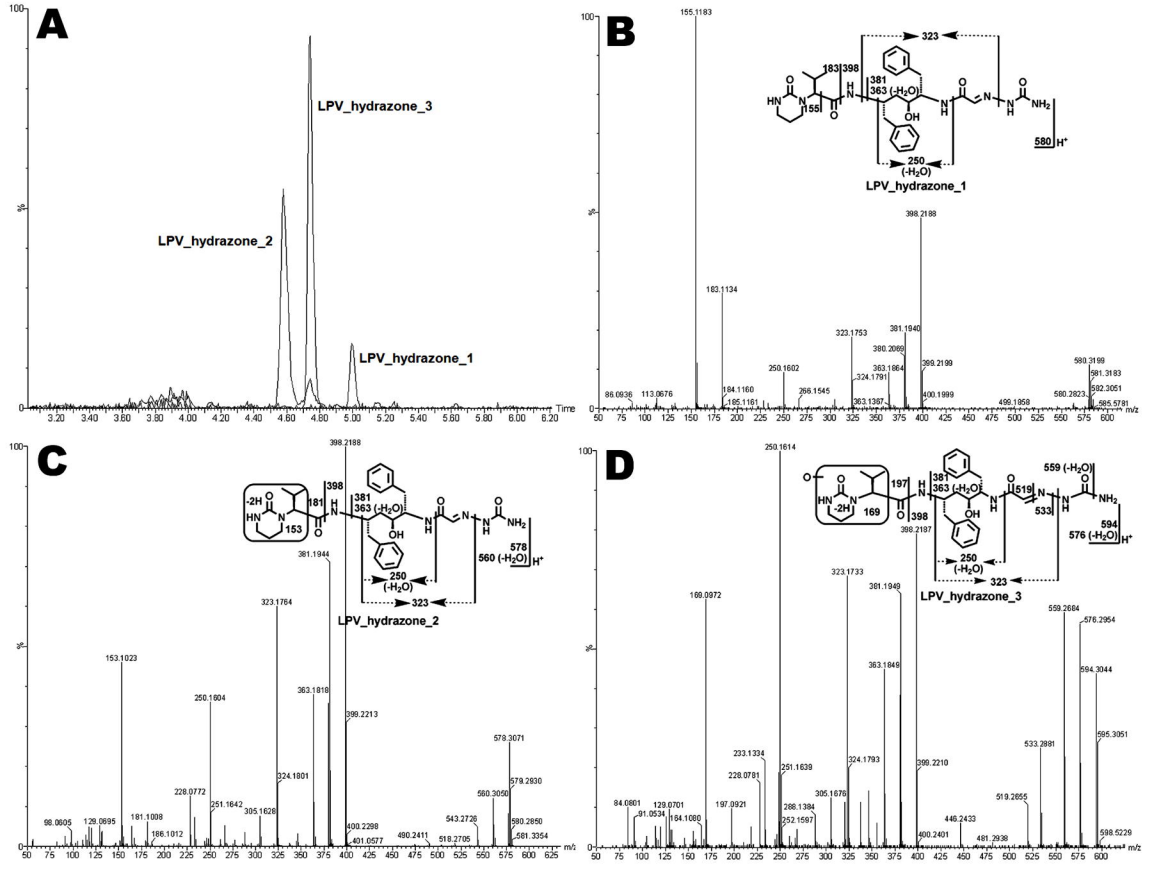
A
LPV_hydrazone_3
LPV_hydrazone_2
LPV_hydrazone_1
Time
B
155.1183
323
183
398
381
363 (-H2O)
55
580 H+
250 (-H2O)
LPV_hydrazone_1
398.2188
163.1134
323.1753
381.1940
380.2069
399.2199
250.1602
363.1864
324.1791
580.3199
581.3183
592.3051
86.0936
113.0676
184.1160
185.1161
266.1545
363.1367
400.1999
499.1858
580.2823
585.5781
m/z
C
398.2188
-2H
153
181
398
381
363 (-H2O)
578
560 (-H2O) H+
250 (-H2O)
323
LPV_hydrazone_2
381.1944
323.1764
153.1023
363.1818
250.1604
399.2213
578.3071
324.1801
579.2830
228.0772
251.1642
305.1628
580.3050
98.0605
129.0695
181.1008
186.1012
400.2299
401.0577
490.2411
543.2728
580.2850
518.2705
581.3354
m/z
D
250.1614
-2H
169
197
381
363 (-H2O)
559 (-H2O)
619
533
594
576 (-H2O) H+
398
398.2197
250 (-H2O)
323
LPV_hydrazone_3
323.1733
381.1949
169.0972
559.2664
576.2954
363.1849
594.3044
595.3051
233.1334
251.1639
228.0781
324.1793
399.2210
533.2891
84.0801
129.0701
91.0534
184.1089
197.0921
288.1384
305.1676
519.2655
252.1597
446.2433
400.2401
481.2938
598.5229
m/z

Figure 4

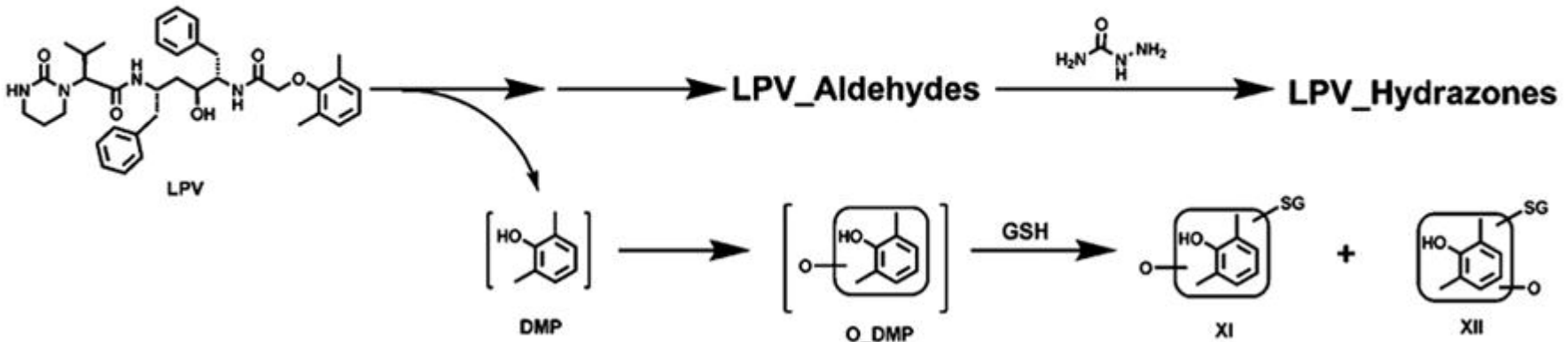

Figure 5

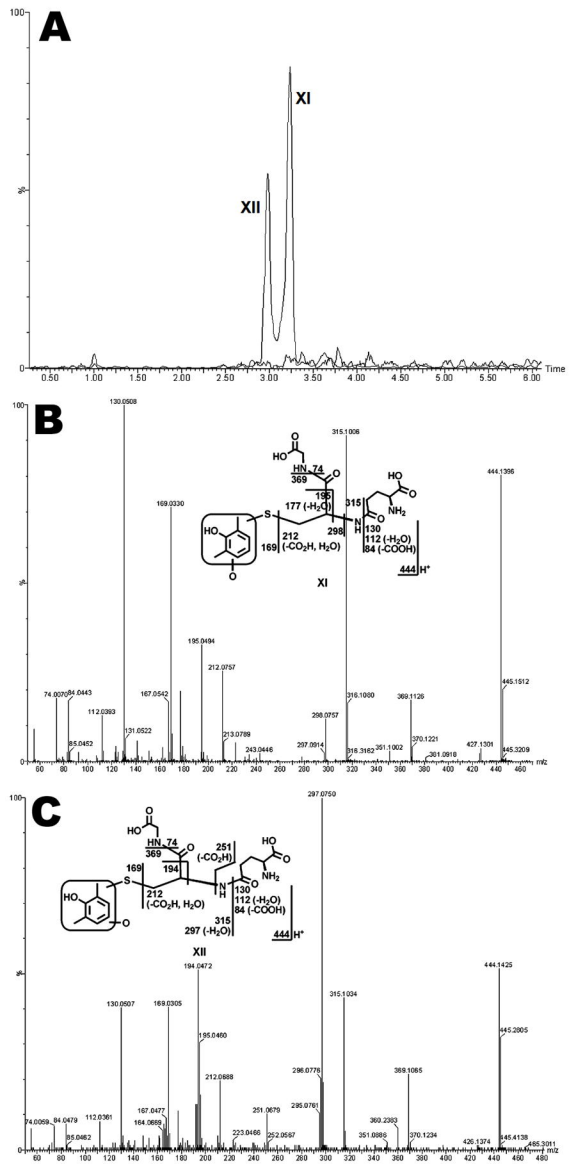

Figure 6

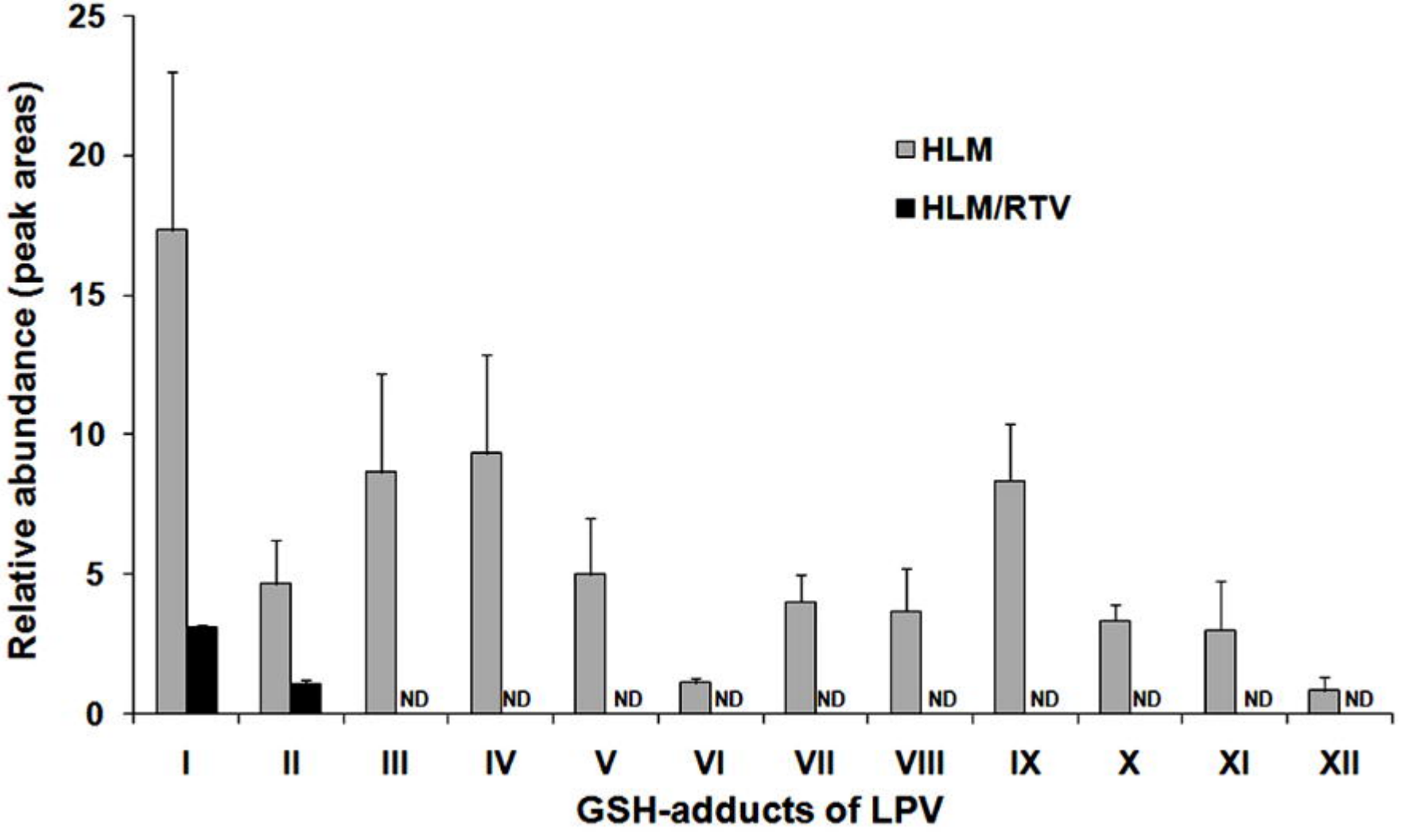
25
20
15
10
5
0
Relative abundance (peak areas)
HLM
HLM/RTV
ND
I
II
III
IV
V
VI
VII
VIII
IX
X
XI
XII
GSH-adducts of LPV

Figure 7

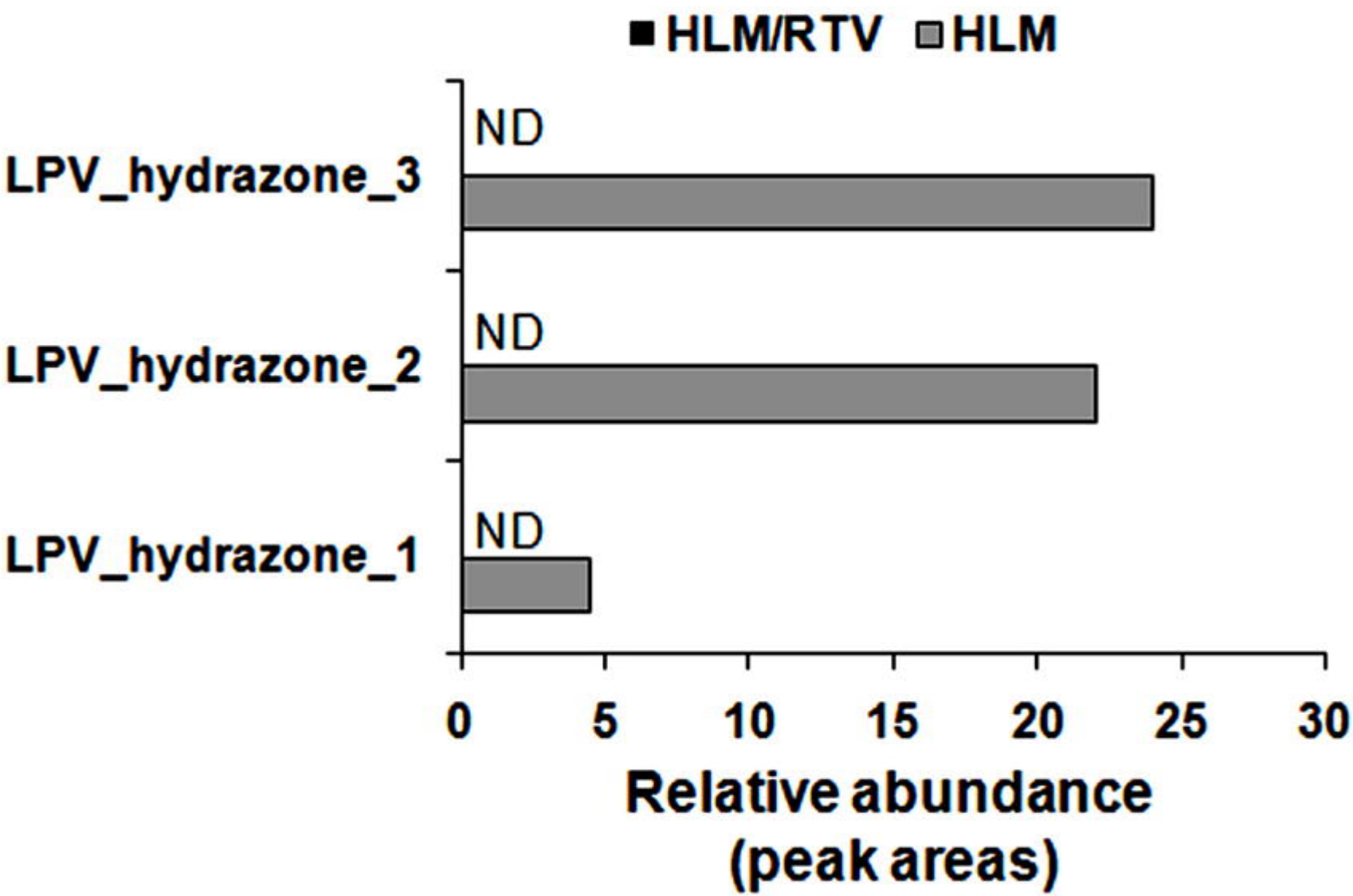
HLM/RTV
HLM
LPV_hydrazone_3
LPV_hydrazone_2
LPV_hydrazone_1
ND
ND
ND
0
5
10
15
20
25
30
Relative abundance
(peak areas)

Figure 8

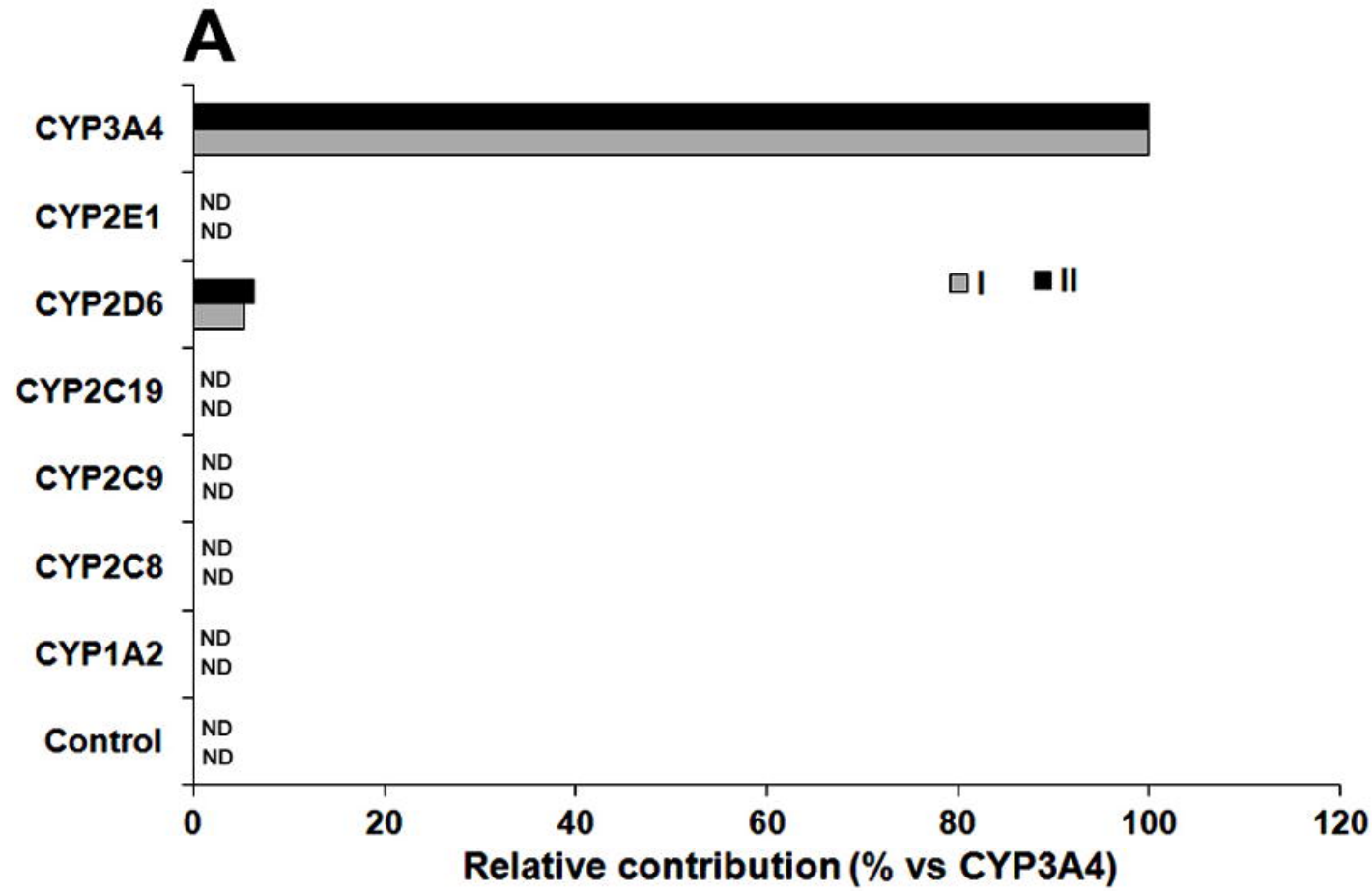
A
CYP3A4
CYP2E1
CYP2D6
CYP2C19
CYP2C9
CYP2C8
CYP1A2
Control
ND
ND
I
II
0
20
40
60
80
100
120
Relative contribution (% vs CYP3A4)

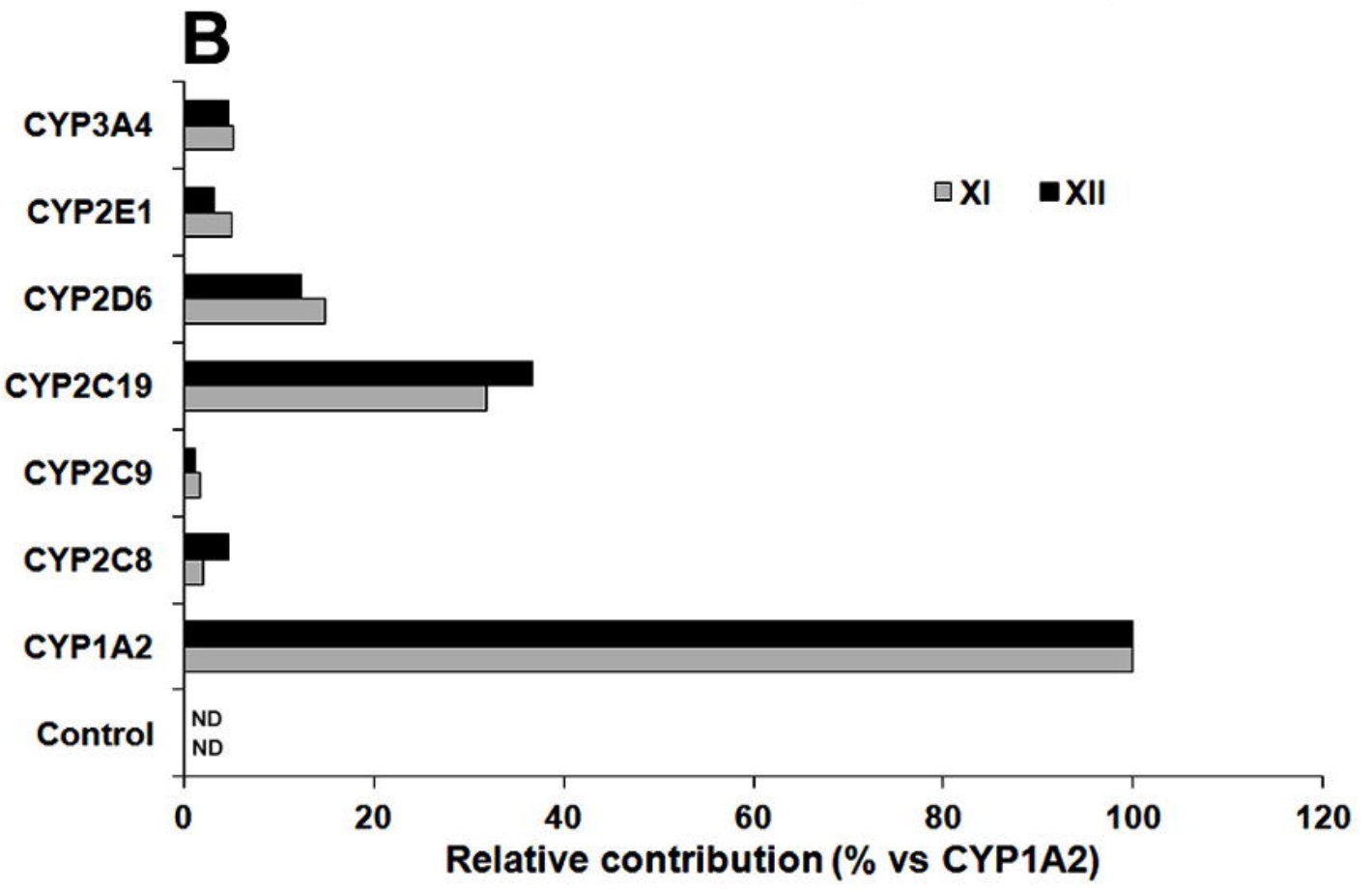
B
CYP3A4
CYP2E1
CYP2D6
CYP2C19
CYP2C9
CYP2C8
CYP1A2
Control
ND
ND
XI
XII
0
20
40
60
80
100
120
Relative contribution (% vs CYP1A2)

Drug Metabolism and Disposition

CPY3A4-mediated lopinavir bioactivation and its inhibition by ritonavir

Feng Li, Jie Lu, and Xiaochao Ma

Department of Pharmacology, Toxicology and Therapeutics, University of Kansas Medical Center

Supplemental Figure 1

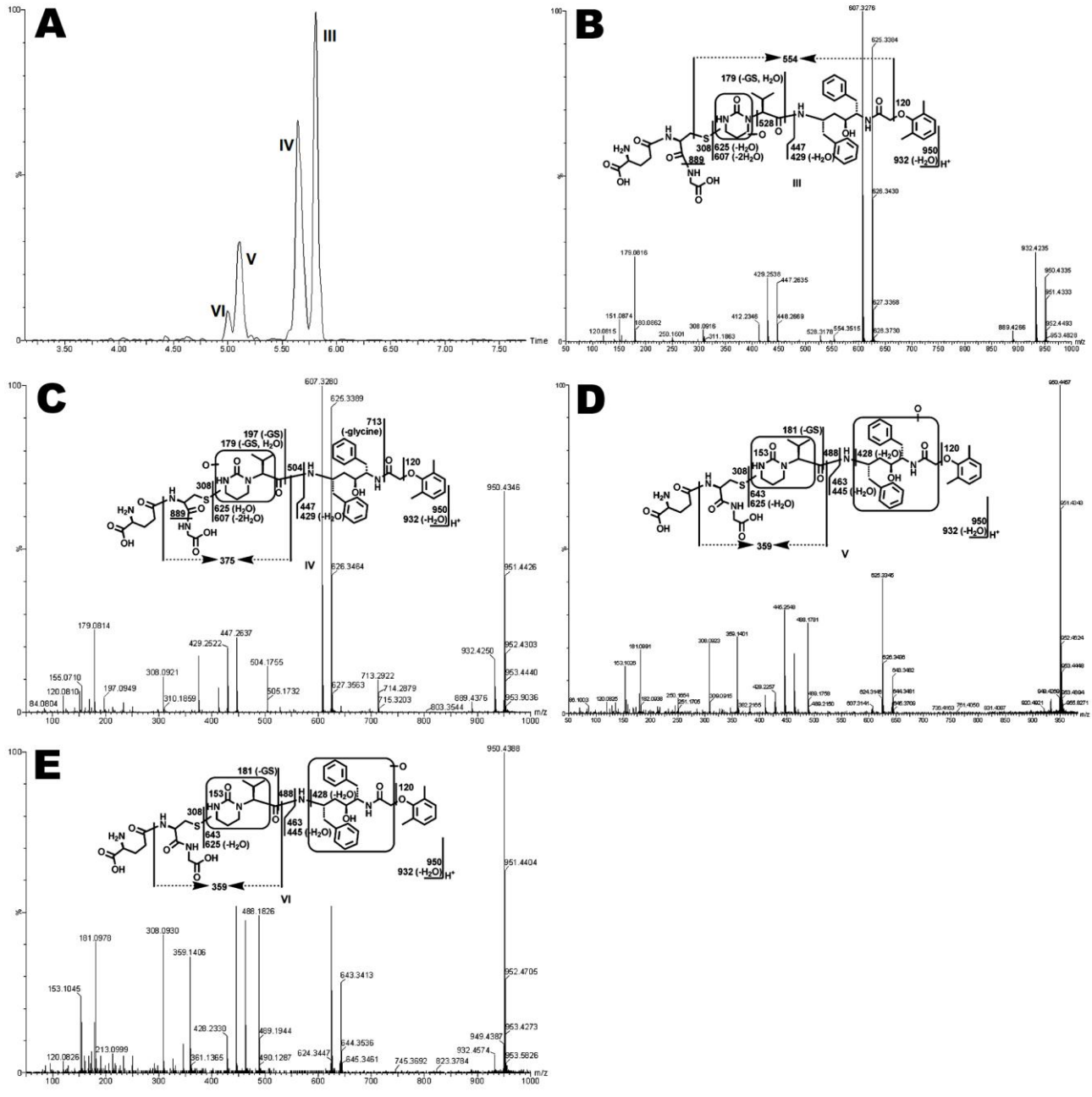

Supplemental Figure 1. The extracted ion chromatograms (A) and MS/MS spectra of LPV adducts III (B), IV (C), V (D), and VI (E). LPV was incubated in HLM containing GSH and analyzed by UPLC-TOFMS. Four monohydroxylated LPV_GSH adducts were identified. Adduct III **(B)**, eluted at 5.81 min, had a protonated molecule

$[M+H]^+$ at *m/z* 950.4335, 16 Daltons higher than that of LPV_GSH adduct. The fragment ions at *m/z* 554.3515 and 528.3178 suggest that the GSH moiety was attached to the encircled unit. The fragment ion at *m/z* 179.0816 suggests that hydroxylation took place in the encircled unit of the molecule. Adduct IV (at a retention time of 5.65 min) corresponded to a protonated molecule $[M+H]^+$ at *m/z* 950.4346, 16 mass units higher than that of LPV_GSH adduct. Adduct IV **(C)** had the same major fragment ions at *m/z* 625.3384, 607.3276, 447.2635, and 429.2538 as those of adduct III. The formation of fragment ions at *m/z* 504.1755 and 375.1332 indicate that the GSH moiety was linked to the encircled unit. The fragment ion at *m/z* 179.0814 suggests that hydroxylation took place in the encircled unit of the molecule. Compared to mass spectra of adducts I and II, the ion at *m/z* 375.1329 is 16 Daltons higher than the ions (*m/z* 359.1408) generated from adducts I and II, which further demonstrates the oxidized position. Adduct V **(D)** was detected at 5.11 min with a protonated molecule $[M+H]^+$ at *m/z* 950.4457. The MS/MS of adduct V produced the fragment ions at *m/z* 643.3482 (loss of GSH), 488.1781, 463.2630, and 359.1410. The fragment ions at *m/z* 488.1781 and 359.1410 indicate that GSH was coupled to the left encircled panel, which consists with the MS/MS spectra of adducts I and II (Figures 2C and 2D). The ion at *m/z* 463.2630 is 16 mass units higher than the ion at *m/z* 447.2668 generated from LPV adducts I and II (Figure 2). The formation of fragment ions at *m/z* 463.2634 and 120.0825 suggest that the oxidation occurred in the right encircled unit. Adduct VI **(E)** was eluted at 5.00 min, having a protonated molecule $[M+H]^+$ at *m/z* 950.4388. Adduct VI had similar mass spectra fragmentation patterns to that of adduct V. The formation of ions at *m/z* 488.1826, 463.2612, and 359.1406 suggest that the GSH adduction and oxidation happened in the same encircled panels like adduct V, but at a different position.

Supplemental Figure 2

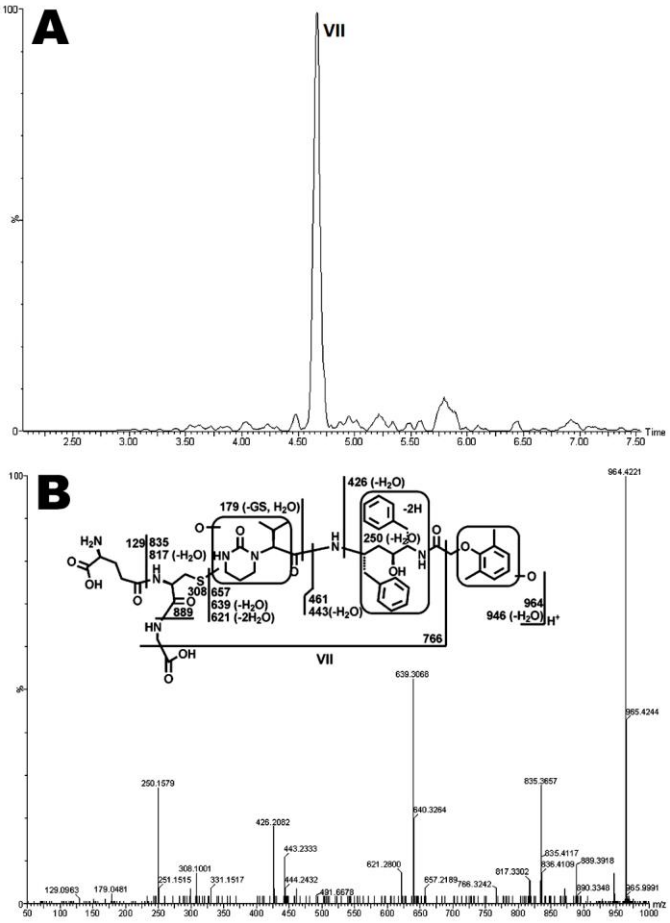

Supplemental Figure 2. The extracted ion chromatogram (A) and MS/MS spectra (B) of LPV adduct VII. LPV was incubated in HLM containing GSH and analyzed by UPLC-TOFMS. LPV adduct VII was detected at 4.66 min, having a mass of $[M+H]^+$ at *m/z* 964.4221. The MS/MS of LPV adduct VII produced fragment ions at *m/z* 835.3657 (loss of pyroglutamic acid), and 639.3068 (loss of GSH and H_2O). The fragmental ions at *m/z* 766.3242 and 179.0481 suggest that one oxidation took place on the 2,6-dimethylphenol moiety and the other one on left encircled panel. In addition, compared to the ions at *m/z* 463.2607 and 445.2548 generated from adducts V and VI, the ions at *m/z* 463.2607 and 443.2333 indicate that the dehydrogenation occurred on the middle encircled panel.

Supplemental Figure 3

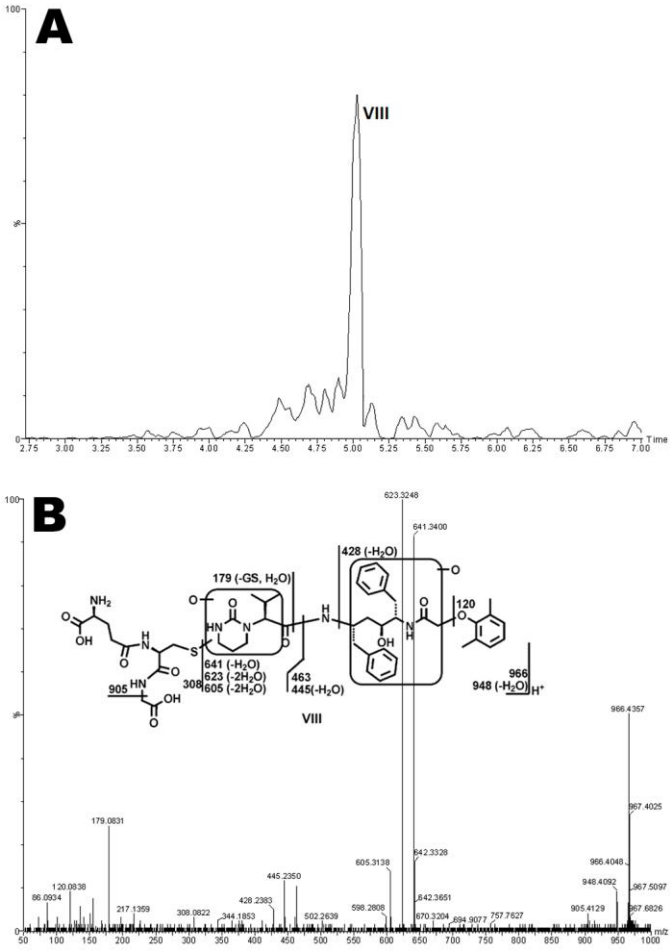

Supplemental Figure 3. The extracted ion chromatogram (A) and MS/MS spectra (B) of LPV adduct VIII. LPV was incubated in HLM containing GSH and analyzed by UPLC-TOFMS. LPV adduct VIII (retention time at 5.03 min) had a mass of $[M+H]^+$ at *m/z* 966.4357. The corresponding MS/MS analysis showed the major fragment ions at *m/z* 948.4092 (loss of H_2O), 641.3400 (loss of GSH and H_2O), and 120.0838 (2,6-dimethylphenol). The fragment ion at *m/z* 463.2536, 428.2350, 179.0831, and 120.0838 suggest that one oxidation happened on the left encircled panel and the other one on the right encircled panel.

Supplemental Figure 4

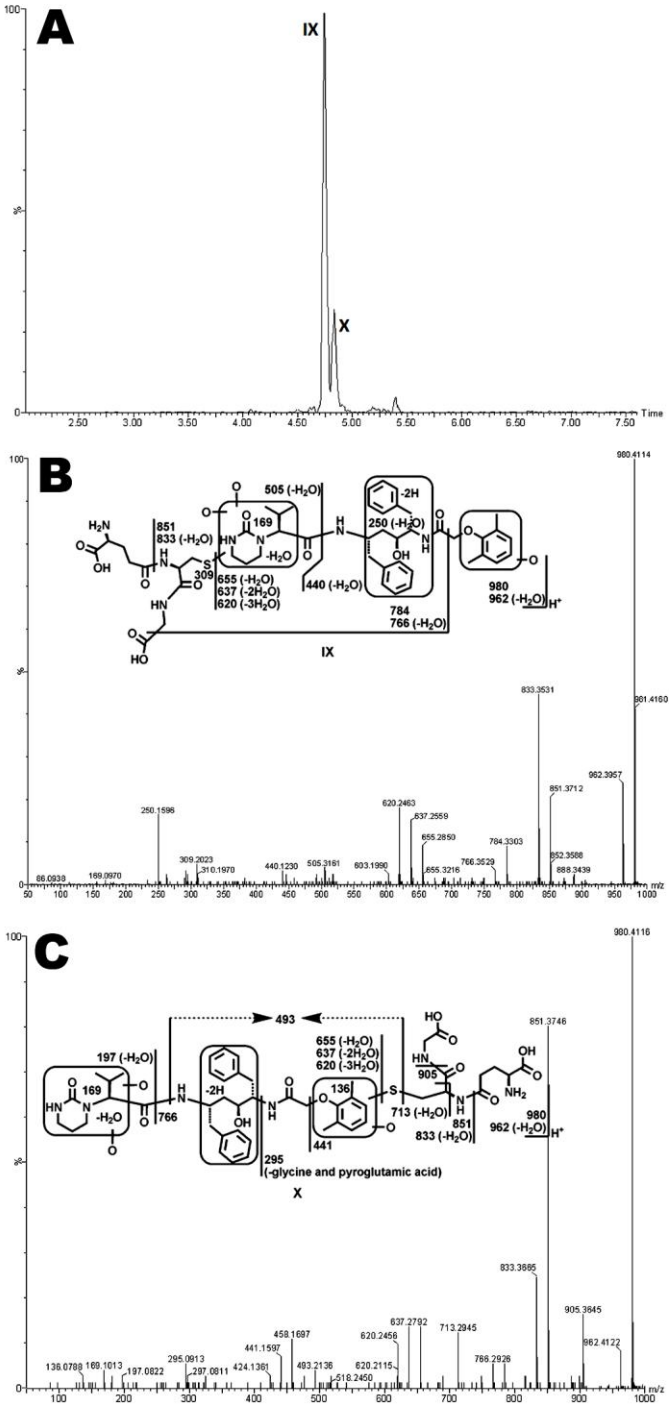

Supplemental Figure 4. The extracted ion chromatograms (A) and MS/MS spectra of IX (B) and X (C). LPV was incubated in HLM containing GSH and analyzed by UPLC-TOFMS. LPV adduct IX **(B)**, eluted at 4.70 min, had a protonated molecule

$[M+H]^+$ at *m/z* 980.4114. MS/MS analysis of LPV adduct V produced daughter ions at *m/z* 962.3957 (loss of H_2O), 851.3712 (loss of pyroglutamic acid), 655.2850 (loss of GSH and H_2O). The fragment ions at *m/z* 784.3303 and 505.3161 suggest that one oxidation occurred in the 2,6-dimethylphenol moiety and dioxidation happened on the left encircled panel. Adduct X **(C)**, eluted at 4.78 min, had a mass of $[M+H]^+$ at *m/z* 980.4116. MS/MS analysis of X produced daughter ions at *m/z* 962.4122 (loss of H_2O), 851.3746 (loss of pyroglutamic acid), 655.2849 (loss of GSH and H_2O). The fragment ions at *m/z* 197.0822 and 136.0788 suggest that dioxidation happened on the left encircled panel and one oxidation occurred in the 2,6-dimethylphenol moiety. The ions at *m/z* 493.2136 and 441.1597 indicate that the GSH attached to the oxidized 2,6-dimethylphenol moiety.